*Thermochimica Acta*, 160 (1990) 233–242
Elsevier Science Publishers B.V., Amsterdam – Printed in The Netherlands

# EFFECT OF IRON CONCENTRATION ON THE THERMAL BEHAVIOUR OF $\gamma$-$Mn_2O_3$

J. PATTANAYAK *

*Materials Science Centre, Central Research Facility, Indian Institute of Technology, Kharagpur 721 302 (India)*

V. SITAKARA RAO **

*Department of Chemistry, Indian Institute of Technology, Kharagpur 721 302 (India)*

H.S. MAITI

*Electro Ceramics Division, Central Glass and Ceramics Institute, Jadavpur, Calcutta 700 032 (India)*

(Received 13 September 1989)

## ABSTRACT

Samples of $\gamma$-$Mn_2O_3$ with various iron contents are obtained by co-precipitation from appropriate amounts of manganese sulphate and ferric nitrate solutions by a concentrated (2.5 N) boiling solution of sodium hydroxide. Thermal analysis, X-ray diffraction and IR spectroscopy of the specimens reveal that the presence of iron in $\gamma$-$Mn_2O_3$ up to 15 to 25 at.% leads to formation of a single phase $\gamma$-$Mn_2O_3$ solid solution, which is partly reduced to $Mn_3O_4$ around 680 °C and finally transforms to the $\alpha$-$Mn_2O_3$ phase on heating at or above 950 °C. With increasing iron concentration beyond 25 at.%, the formation of a ferrite phase has been detected in addition to the $\gamma$-$Mn_2O_3$ solid solution. However, this ferrite phase is thermally unstable and breaks down on heating around 600 °C.

## INTRODUCTION

Thermal transformations of pure and of mixed oxides and of hydroxides of different metal ions have been studied by various investigators [1–4], and it is observed that isomorphous substitution of lattice metal ions with foreign metal ions can cause a shift in the peak temperature, as the foreign ion can promote or impair the stability of the particular phase present. There may be three different effects if a foreign metal ion is present in the solution during the precipitation of a compound [1]. They are: (i) the ion

---

* Author to whom correspondence should be addressed.

** Professor (retired).

0040-6031/90/$03.50

may retard the crystallization; (ii) it may influence the type of compound formed; (iii) it may lead to the formation of a substituted solid solution. Chalyi and Shor [2] and Rajendran [3] observed a shift in the peak temperature of nickel hydroxide due to solid solution formation with $Mg^{2+}$, $Zn^{2+}$ or $Fe^{3+}$ as foreign ion. Similar results have also been reported by Prasad [4] for the copper–iron mixed oxide system. Not only solid solution formation, but also factors such as mutual interaction [5] of various components present and the protection of one metal component by the other, can cause a shift in the peak position [6,7].

The $\gamma$ form of manganese sesquioxide ($Mn_2O_3$) is a very unstable oxide and has been reported not to occur in nature [8,9]. Since both $\gamma$-$Mn_2O_3$ and $Mn_3O_4$ have nearly identical crystal structures [10] it is difficult to identify them individually by such experimental techniques as X-ray diffraction or IR spectroscopy. Like other manganese oxides, $\gamma$-$Mn_2O_3$ cannot be prepared easily from aqueous $Mn^{2+}$ solution or by oxidation or reduction of a lower or higher state of manganese oxide, respectively. Very little research work has been reported on the preparation and thermal behaviour of $\gamma$-$Mn_2O_3$ (see ref. 11) and no literature has been found on the preparation and thermal behaviour of $\gamma$-$Mn_2O_3$ containing various concentrations of iron ions.

In our previous work [11], a special technique for preparation and identification of a $\gamma$-$Mn_2O_3$ specimen, along with its thermal behaviour, was reported. In the present work, samples of $\gamma$-$Mn_2O_3$ with different iron concentrations have been prepared by a co-precipitation method. Attempts have been made to establish the maximum iron concentration up to which iron forms a solid solution with $\gamma$-$Mn_2O_3$ and, finally, the solid solution effect on the thermal stability of $\gamma$-$Mn_2O_3$ is discussed in detail.

## EXPERIMENTAL

Specimens of $\gamma$-$Mn_2O_3$ with different iron concentrations were prepared by a co-precipitation method. The appropriate amounts of ferric nitrate (GR) and manganese sulphate (GR) were dissolved in 250 ml of distilled water. This mixed metal ion solution was then added to 250 ml of freshly prepared boiling 2.5 N sodium hydroxide (GR) solution. The solution was continuously stirred during precipitation, and constant pH of the solution was maintained throughout the experiment, with further addition of sodium hydroxide solution. The separated precipitate was washed repeatedly with distilled water until the washings were free from adsorbed impurity ions, and solid was then dried in air. The absence of an appreciable amount of sodium in the precipitates was confirmed by using a digital flame photometer.

TABLE 1

Sample code with corresponding content (at.%) of iron

| Code | Nominal at.% of iron | Actual at.% of iron [a] |
|---|---|---|
| S1 | 0 | 0 |
| S2 | 10 | 8.1 |
| S3 | 15 | 14.9 |
| S4 | 25 | 24.9 |
| S5 | 35 | 34.9 |
| S6 | 55 | 53.0 |

[a] Compositions determined by chemical analyses.

The elemental compositions of manganese and iron present in the specimens were analysed quantitatively. Initially, the manganese and iron ions were separated from their mixed composition by the basic acetate method [12]. The separation depends upon the fact that solutions of acetates of iron are decomposed when heated and the insoluble basic acetate is precipitated, whereas the acetate of manganese remains undecomposed when boiled for a short time

$$Fe(C_2H_3O_2)_3 + 2HOH \rightarrow 2HC_2H_3O_2 + Fe(OH)_2C_2H_3O_2$$

After separation, the basic acetate of iron was dissolved in dilute hydrochloric acid and the amount of iron was determined by the Zimmermann–Reinhardt method [13]. The manganese present in the filtrate as the bivalent ion was determined by the bismuthate method [13].

The composition of elements present in the specimens are expressed in terms of atoms per cent, thus

$$\text{at.\% of Fe} = (\text{no. of Fe atoms})/(\text{total no. of atoms of manganese and iron}) \times 100$$

The sample codes and corresponding compositions (both theoretical and experimentally observed values) are given in Table 1.

Thermal analyses of oven dried samples were carried out in a Stanton Redcraft model STA-780 thermal analyser using a suitable quantity of the sample (20 to 25 mg).

The IR spectra of the samples were taken with a Perkin–Elmer model 983 spectrophotometer in the range 200–4000 $cm^{-1}$ by using either potassium bromide or polythene pellets.

X-ray diffraction patterns of the samples were obtained by using a JEOL type JDX-8P X-ray diffractometer operated at 30 kV and 15 mA; Fe $K\alpha$ radiation was used as the X-ray source.

## RESULTS AND DISCUSSION

It has already been established by Pattanayak et al. [11] that, on heating, $\gamma$-$Mn_2O_3$ slowly becomes converted to $Mn_3O_4$ and remains as a mixture of

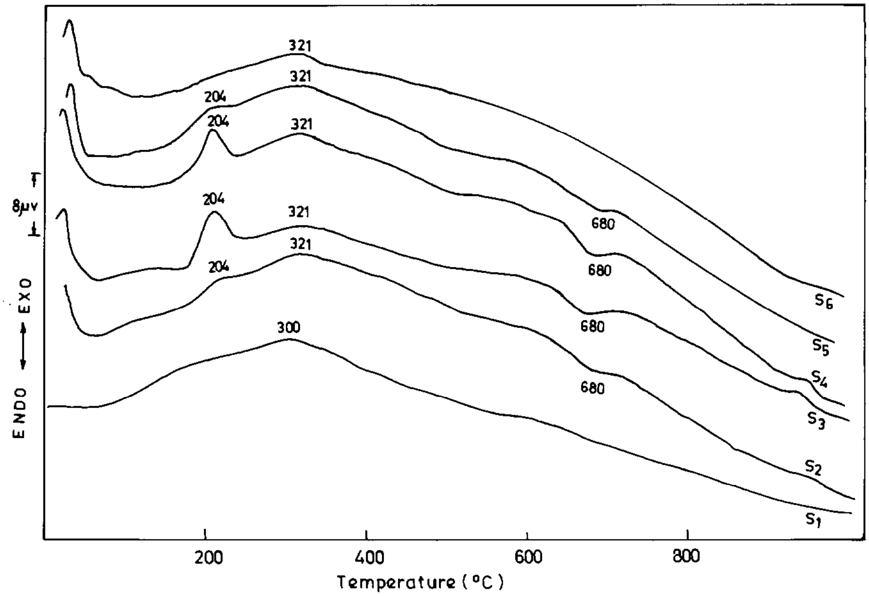

Fig. 1. DTA curves of samples of $\gamma$-$Mn_2O_3$ with various iron concentrations.

$\gamma$-$Mn_2O_3$ and $Mn_3O_4$ at 800 °C. The mixture finally forms a single phase of $Mn_3O_4$ above 1100 °C through an intermediate phase of $\alpha$-$Mn_2O_3$. The results of differential thermal analyses (DTA) of samples of $\gamma$-$Mn_2O_3$ containing 0–53 at.% of iron (S1–S6) are given in Fig. 1. Thermogravimetric (TG) plots for the same specimens are presented in Fig. 2. All the samples except S1 (pure $\gamma$-$Mn_2O_3$) show a distinct but broad endothermic peak, starting at around 35 °C and extending up to a maximum of 320 °C (in the case of S6). This endotherm corresponds to the removal of different types of bound water [14] from the structure of primary particles. It may be noted from Fig. 1 that the temperature as well as width of the first endothermic peak vary significantly with increasing concentration of iron. The increased width of the endotherm with increasing amount of iron added to the specimen of $\gamma$-$Mn_2O_3$ (S1) establishes the fact that the presence of iron ions in the lattice of $\gamma$-$Mn_2O_3$ favours the adsorption of water molecules, which the sample loses stepwise over a wide range of temperature. A significant amount of this weight loss takes place around 200 °C (Fig. 2), and the calculation of weight loss within the temperature range 30–250 °C (from the TG curve) for these samples indicates that the weight loss is maximum for sample S3 and minimum for S1 and S6 (Fig. 3). It may be noted in Figs. 1 and 2 that the weight loss around 200 °C is also associated with an exothermic peak in the DTA curve. These effects are particularly strong in samples containing appreciable amounts of iron, and this peak is nearly absent for the pure $\gamma$-$Mn_2O_3$ specimen (S1). However, the intensity of the exothermic peak gradually increases with iron concentration up to ca. 15

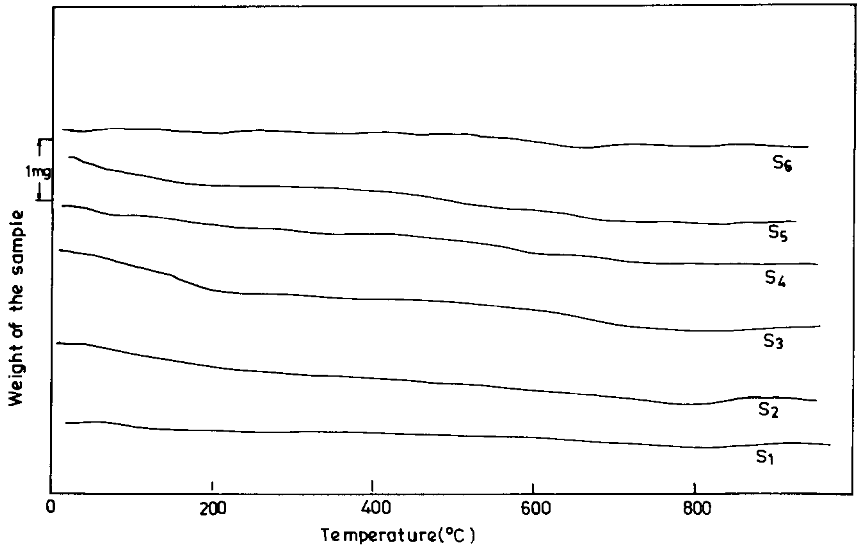

Fig. 2. TG curves of samples of $\gamma$-$Mn_2O_3$ with various iron concentrations.

at.% (S3) and decreases with further addition of iron, finally disappearing in the sample containing 53 at.% of iron (S6).

X-ray diffraction (XRD) patterns of samples S1–S3 heated at different temperatures up to 600 ° C show only $\gamma$-$Mn_2O_3$ lines (Fig. 4), beyond which they gradually convert to the lines of the $\alpha$-$Mn_2O_3$ phase around 1000 ° C. Air-dried samples of S5 and S6 show the formation of manganese ferrite as a second phase along with the $\gamma$-$Mn_2O_3$ phase (Fig. 5). This ferrite phase decomposes on heating the sample around 600 ° C. Sample S4 shows practically the same behaviour as S5 and S6, except that the X-ray lines of the ferrite phase are not observed in the air-dried sample, possibly because it is present in insignificant amount.

IR spectra of the air-dried mixed oxide samples S1–S6 show absorption peaks around 3400 $cm^{-1}$ and 1630 $cm^{-1}$, which are due to OH stretching

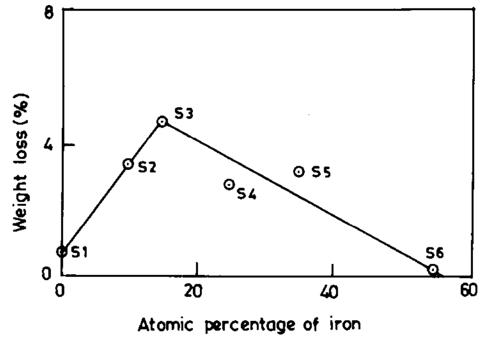

Fig. 3. Percentage weight loss of samples (S1–S6) heated to 250 ° C.

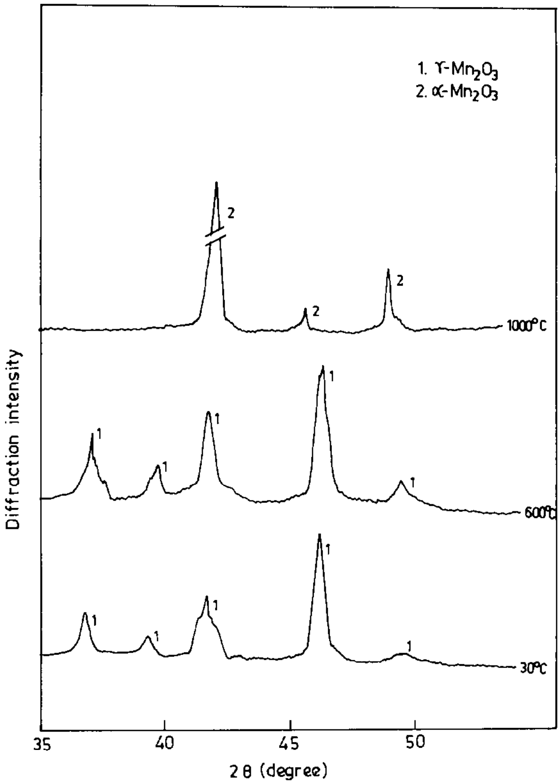

Fig. 4. X-ray diffraction patterns of sample S2 heated at different temperatures.

and bending vibrations of surface water. The absorption peak of the deformation vibration of the OH group i.e. that at 880 $cm^{-1}$ (in S1), shows a shift to higher frequency regions on increasing the iron concentration up to 15 at.%, but a shift to lower frequency takes place on further increase of iron content up to 53 at.% (S6). Comparing the IR transmittance peaks of S1 with those of different manganese oxides in the low frequency range, as given by Gattow and Glemser [15], it has already been established that the sample S1 consists of $\gamma$-$Mn_2O_3$ [11]. Peaks similar to those of S1 are observed with all the samples from S2–S6 except for slight shifts in the maxima (Fig. 6). These peaks indicate the presence of $\gamma$-$Mn_2O_3$ (either pure or as a solid solution with iron) in these samples. It may be noted that, with increasing concentration of iron up to 24 at.% (i.e., S4), the intensities of the absorption peaks decrease gradually while their maxima shift slightly towards the lower frequency range (Table 2). In particular, the intensity of the peak around 415 $cm^{-1}$ decreases quite significantly on the addition of iron ions, and almost vanishes in S4 (24 at.% of iron). With further addition of iron up to 53 at.%, this peak reappears in the spectra of S5 and S6, but the positions of the maxima are shifted to higher frequencies.

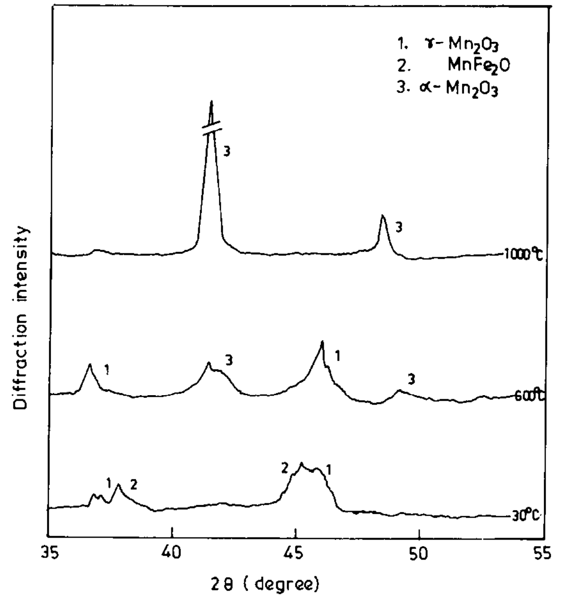

Fig. 5. X-ray diffraction patterns of sample S5 heated at different temperatures.

All the results mentioned above indicate a direct correlation between the extent of weight loss, the change of intensity of the exotherm around 200 ° C, and the shift of the IR bands. It is difficult to visualise that removal of moisture alone could give rise to such changes in these specimens. It may be assumed that the moisture removal is also associated with some kind of unidentified structural change which leads to an exotherm in the DTA curve and shifts of IR bands. Structural change may be due to solid solution formation in air-dried specimens. On adding iron to pure $\gamma$-$Mn_2O_3$, the $Fe^{3+}$ ion displaces the $Mn^{3+}$ ion to form a solid solution of $\gamma$-$Mn_2O_3$ up to at least 24 at.% of iron, beyond which such formation decreases, with associated decrease of moisture loss, and the iron and manganese ions finally form a ferrite phase. The formation of a $\gamma$-$Mn_2O_3$ solid solution is thus responsible for shifting of the IR peaks towards the low frequency range. Formation of a ferrite phase increases as the intensity of the exothermic peak at 200 ° C decreases, along with the shifting of IR peaks to the high frequency region. It may also be noted from Fig. 1 that a broad exotherm around 320 ° C exists in all the specimens, irrespective of the iron concentration; all specimens thus contain a common phase, normallly $\gamma$-$Mn_2O_3$. This peak, which is not associated with appreciable weight loss of moisture, must be related to some sort of structural rearrangement of the $\gamma$ phase, the exact nature of which remains unknown.

In addition to these endo- and exothermic peaks, the thermograms of Fig. 1 also contain one more endothermic peak at 680 ° C and an exothermic peak around 950 ° C. Both of these peaks are almost nonexistent in sample

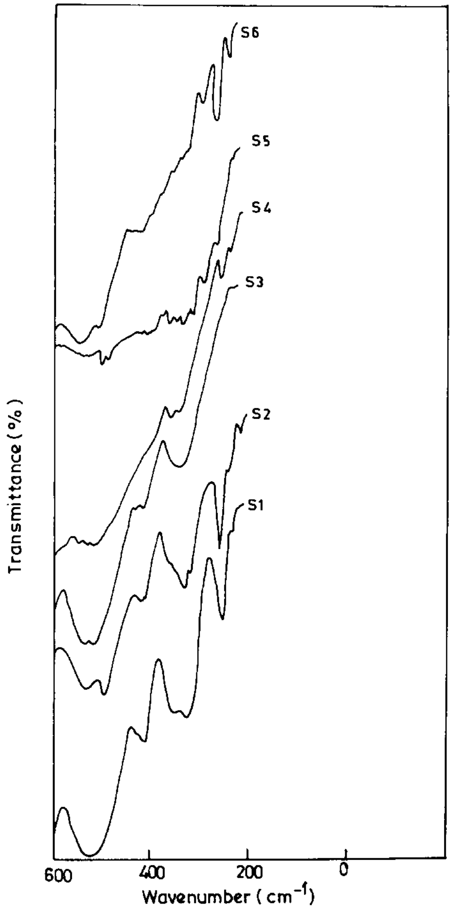

Fig. 6. IR spectra of samples (S1–S6) dried at room temperature.

TABLE 2

IR bands of S1–S6 dried at room temperature (in low wavenumber range)

| Sample code | Transmittance peaks ($cm^{-1}$) | | | | | |
|---|---|---|---|---|---|---|
| | I | II | III | IV | V | VI |
| S1 | 570 | 435 | 380 | 270 | | |
| S2 | 570 | 430 | 375 | 270 | | |
| S3 | 570 | 420 | 370 | | | |
| S4 | 560 | 415<br>(V.W.) | 360 | | | |
| S5 | 575 | 430 | 360 | 285 | 250<br>(V.W.) | 230<br>(V.W.) |
| S6 | 575 | 435 | 360 | 290 | 260<br>(V.W.) | 240<br>(V.W.) |

V.W., Very weak.

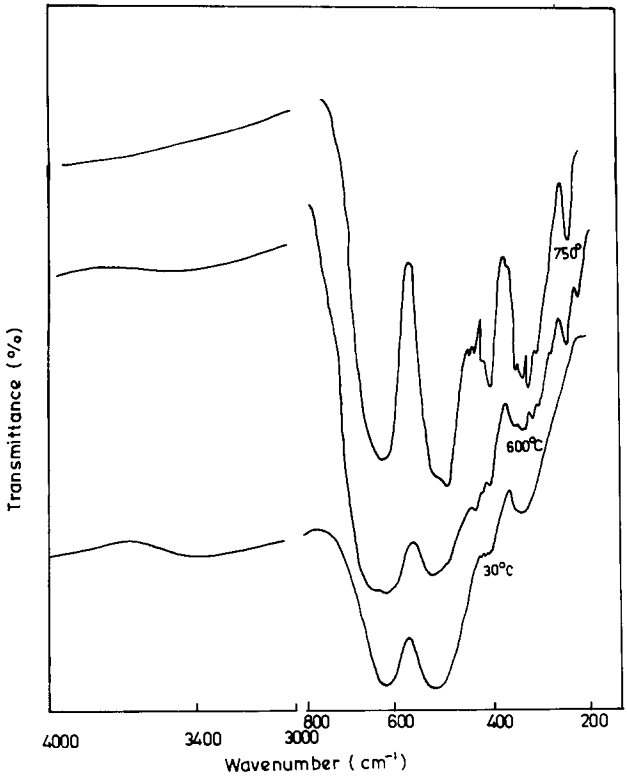

Fig. 7. IR spectra of sample S3 heated at different temperatures.

S1 but are distinctly present in samples of iron concentration up to 15 to 25 at.%. At higher concentrations of iron these peaks gradually disappear. It may be noted in Fig. 2 that the low temperature endothermic peak is associated with a small weight loss and the high temperature exothermic peak is associated with a nearly equal weight gain. In order to get a clear idea of this effect, a detailed study has been made of the IR spectra of sample S3 heated at various temperatures (Fig. 7). It is observed that IR bands of the sample heated to 600 ° C show a pattern the same as that of $\gamma$-$Mn_2O_3$, but at 700 ° C the spectrum shows two almost equally intense characteristic transmission peaks at 570 and ca. 430 $cm^{-1}$. This suggests the formation of a mixture of $\gamma$-$Mn_2O_3$ and $Mn_3O_4$ [11] which cannot be differentiated by XRD studies. From this observation it is clear that a part of the $\gamma$-$Mn_2O_3$ solid solution reduces to $Mn_3O_4$ around 680 ° C, which along with the remaining part of the $\gamma$-$Mn_2O_3$ solid solution is converted to an $\alpha$-$Mn_2O_3$ solid solution (Fig. 4) on further heating to ca. 950 ° C and above. The extent of these reduction and oxidation processes increases with a small addition of iron ions, becomes maximum for samples S3 and S4, gradually reduces with further addition of iron, and finally leads to the formation of manganese ferrite.

## REFERENCES

1 U. Schwertmann, J. Soil Sci., 128 (1979) 195.
2 V.P. Chalyi and O.I. Shor, Ukr. Khim. Zh., 27 (1961) 7.
3 S. Rajendran, Ph.D. Thesis, Indian Institute of Technology, Kharagpur, 1983.
4 S.V.S. Prasad, Ph.D. Thesis, Indian Institute of Technology, Kharagpur, 1984.
5 C. Duval, Comprehensive Analytical Chemistry, Vol. 7, Elsevier, New York, 1976.
6 W.O. Milligan and B.G. Holmes, J. Phys. Chem., 57 (1953) 11.
7 W.O. Milligan and L. Merten, J. Phys. Chem., 50 (1946) 465.
8 O. Bricker, Am. Mineral., 50 (1965) 1296.
9 T.E. Moore, M. Ellis and P.W. Selwood, J. Am. Chem. Soc., 72 (1950) 856.
10 W.C. Vosburgh, J. Electrochem. Soc., 106 (1959) 839.
11 J. Pattanayak, V. Sitakara Rao and H.S. Maiti, Thermochim. Acta, 153 (1989) 193.
12 W.W. Scott, Standard Methods of Chemical Analysis, Vol. 1, Lancaster Press, Lancaster 1955, p. 558.
13 F.P. Treadwell and W.T. Hall, Analytical Chemistry, Vol. 2, Wiley, New York, 1948, pp. 545, 551.
14 J.A. Lee, C.E. Newnham and F.L. Tye, J. Colloid Interface Sci., 42 (1973) 370.
15 G. Gattow and O. Glemser, Z. Anorg. Allg. Chem., 309 (1961) 20.